Available online at www.sciencedirect.com
ScienceDirect
Polyhedron 26 (2007) 4397–4410
POLYHEDRON
www.elsevier.com/locate/poly

Syntheses, supramolecular structures and properties of six coordination complexes based on 5-sulfosalicylic acid and bipyridyl-like chelates

Jiang-Feng Song [a], Yan Chen [a], Zhi-Gang Li [b], Rui-Sha Zhou [a], Xiao-Yu Xu [a], Ji-Qing Xu [a,*], Tie-Gang Wang [a]

[a] College of Chemistry and State Key Laboratory of Inorganic, Synthesis and Preparative Chemistry, Jilin University, Changchun, Jilin 130023, PR China
[b] Changchun Institute of Applied Chemistry, Chinese Academy of Sciences, Changchun 130022, PR China

Received 22 January 2007; accepted 22 May 2007
Available online 8 June 2007

Abstract

Six new complexes constructed by 5-sulfosalicylic acid and bipyridyl-like ligands (2,2′-bipy and 1,10-phen), namely $[Cu_4(OH)_2(ssal)_2(phen)_4 \cdot 7H_2O]$ (**1**), $[Cu_4(OH)_2(ssal)_2(bipy)_4 \cdot 2H_2O]$ (**2**), [Cd(Hssal)(bipy)] (**3**), $[Cd(HL)_2(phen)_2]$ (**4**), $[Cr(ssal)(bipy)(H_2O)_2 \cdot 2H_2O]$ (**5**) and $[Cr(ssal)(phen)_2]$ (**6**) (H_3ssal = 5-sulfosalicylic acid, H_2L = *p*-hydroxybenzenesulfonic acid, bipy = 2,2′-bipy, phen = 1,10-phen) were prepared under hydrothermal conditions and their structures were determined by single-crystal X-ray diffraction. Complexes **1** and **2** are both tetranuclear copper complexes with a stepped topology. In complex **3**, a new coordination mode of the $Hssal^{2-}$ group is reported in this work. During the synthetic process of complex **4**, *in situ* decarboxylation of 5-sulfosalicylic acid into *p*-hydroxybenzenesulfonic acid is involved. Two chromium 5-sulfosalicylates (**5** and **6**) are reported for the first time. These new complexes display different supramolecular structures by O–H···O, C–H···O hydrogen bonds as well as π···π, C–H···π and O···π interactions. The results of magnetic determination show that ferromagnetic interactions exist in complex **1**, however, antiferromagnetic interactions exist in **2**.

Keywords: Crystal structure; Hydrothermal synthesis; 5-Sulfosalicylic acid; Magnetic analysis

1. Introduction

Since 1989, the definition of crystal engineering was provided by G.R. Desiraju as "the understanding of intermolecular interactions in the context of crystal packing and in the utilization of such understanding in the design of new solids with desired physical and chemical properties" [1]. The rational design and construction of novel supramolecular materials based on discrete or polymeric metal–organic coordination complexes have garnered considerable interest owing to their intriguing topologies and potential for use as functional materials [2,3]. An important synthetic method for design and tailor-making of such supramolecular materials utilizes suitable organic ligands that can coordinate to metal ions through one or more primary coordination sites, whilst at the same time can participate in additional bonding interactions (hydrogen bonding or other molecular contacts) at peripheral sites. An advantage of this method is that it may combine the flexibility of the weaker interactions with the strength of coordination bonding. This method has been widely employed in polycarboxylate ligands, which have proven to be particularly effective in the formation of both extended hydrogen bonded networks and coordination complexes [4,3e]. The choice of 5-sulfosalicylic acid (H_3ssal) can be attributed to the following reasons: (1) it possesses versatile coordination modes (Chart 1) and has the ability to construct a

* Corresponding author. Tel.: +86 431 8499132; fax: +86 431 8499158.
E-mail address: xjq@mail.jlu.edu.cn (J.-Q. Xu).

0277-5387/$ - see front matter © 2007 Elsevier Ltd. All rights reserved.
doi:10.1016/j.poly.2007.05.037

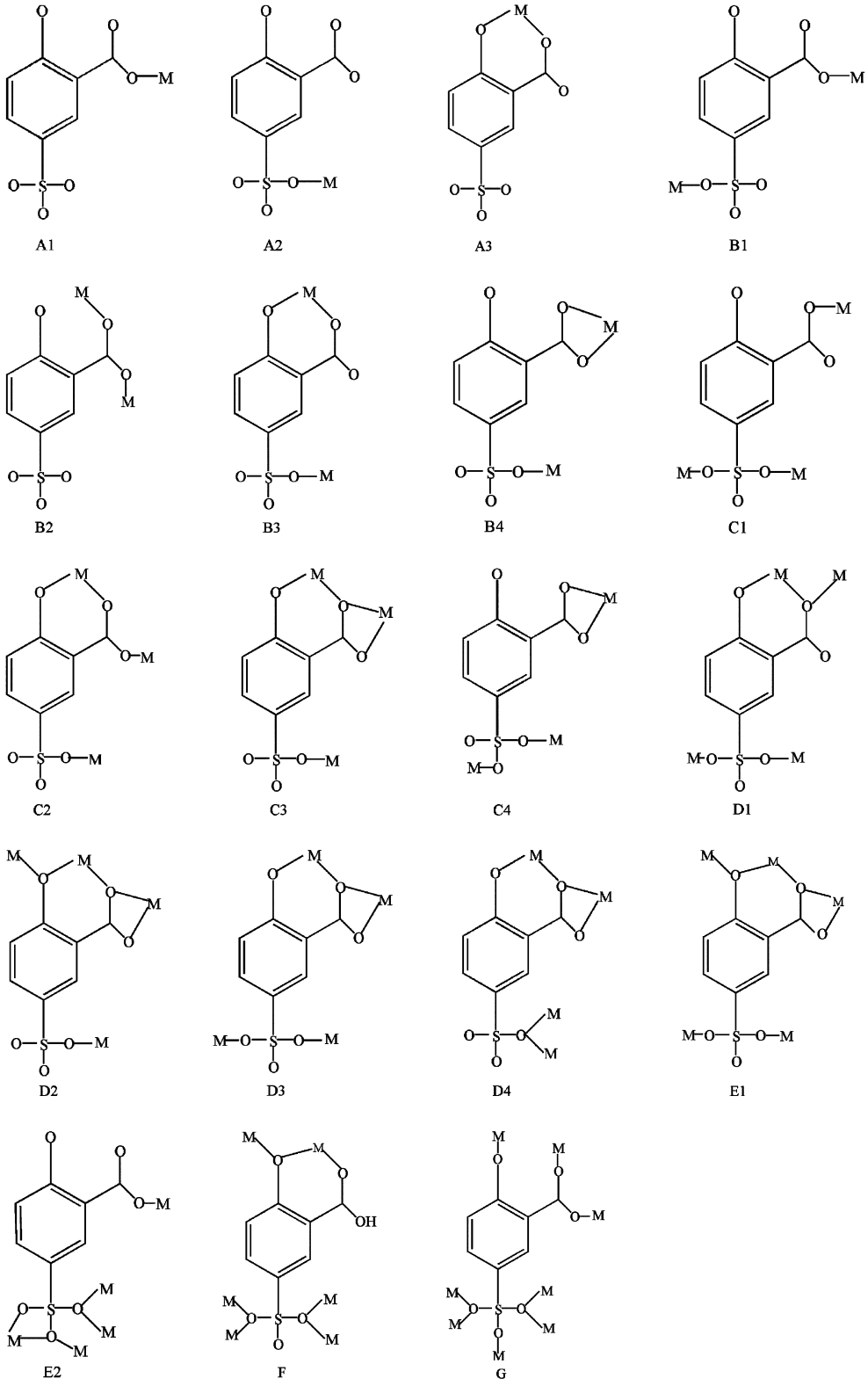

Chart 1. Coordination modes of 5-sulfosalicylates in recent reports (A, B, C, D, E, F, G denote that the 5-sulfosalicylate ligand acts as μ_1, μ_2, μ_3, μ_4, μ_5, μ_6, μ_8 connectors to link metal ions, respectively).

novel metal–organic supramolecular network through specific and directional hydrogen bonds as well as π–π stacking due to the presence of aryl rings [5–7], (2) 5-sulfosalicylic acid has been found to have biological activity and its metal complexes with Cu(II), Ni(II), Co(II), Mn(II), Fe(II), Zn(II) and VO(II) exhibit antimicrobial activity

stronger than that of the free ligand [5b,8]. In order to avoid the formation of higher dimensional coordination networks, polycyclic aromatic chelating ligands such as 2,2′-bipyridyl (2,2′-bipy) and 1,10-phenanthroline (1,10-phen) were introduced based on the following considerations: (1) chelating bipyridyl-like ligands may provide supramolecular recognition sites for π–π, C–H···π stacking and C–H···O hydrogen bonding to form interesting supramolecular structures [4b,4f,9], (2) the conjugated π systems containing (hetero) aromatic rings are currently of interests in the development of fluorescent materials [10].

In order to understand the coordination chemistry of H_3ssal and to prepare new supramolecular materials with intriguing structures and potential physical properties, we have recently focused our research on coordination complexes based on 5-sulfosalicylic acid and chelating bipyridyl-like ligands. Here, we report the syntheses and crystal structures of six new complexes, namely, $[Cu_4(OH)_2(ssal)_2(phen)_4 \cdot 7H_2O]$ (**1**), $[Cu_4(OH)_2(ssal)_2(bipy)_4 \cdot 2H_2O]$ (**2**), [Cd(Hssal)(bipy)] (**3**), $[Cd(HL)_2(phen)_2]$ (**4**), $[Cr(ssal)(bipy)(H_2O)_2 \cdot 2H_2O]$ (**5**) and $[Cr(ssal)(phen)_2]$ (**6**), together with the magnetic properties of complexes **1** and **2**. The crystal structures of complexes Mn(Hssal)$(bipy)_2(H_2O) \cdot 2H_2O$ (**7**) [6b] and Zn(Hssal)$(bipy)(H_2O)_2$ (**8**) [7d] were reported previously. The results demonstrate that the discrete or polymeric complexes may build up higher network connectivity through π–π stacking, C–H···π, O···π and hydrogen-bonding interactions including weak C–H···O contacts.

2. Experimental

2.1. Materials and physical measurements

All chemicals purchased were of reagent grade and were used without further purification. Elemental analyses (C, H, N) were performed on a Perkin–Elmer 240C elemental analyzer. IR spectra were measured on a Perkin–Elmer Spectrum One FT-IR spectrometer using KBr pellets. Magnetic measurements were obtained using an MPMS-XL magnetometer at H = 1000 Oe in the temperature range 5–300 K. The magnetic susceptibility data were corrected for the diamagnetism of the constituent atoms using Pascal's constants.

2.2. Syntheses of the complexes

2.2.1. $Cu_4(OH)_2(ssal)_2(phen)_4 \cdot 7H_2O$ (*1*)

A mixture of $CuSO_4 \cdot 5H_2O$ (0.131 g, 0.5 mmol), 5-sulfosalicylic acid (0.130 g, 0.5 mmol), phen (0.103 g, 0.5 mmol), KOH (0.062 g, 1.1 mmol) and water (15 ml) was stirred for 30 min at room temperature, transferred to and sealed in a 25 ml Teflon-lined stainless steel reactor, and then heated at 150 °C for 72 h. Upon cooling to room temperature, the dark green crystals that were obtained were filtered and washed with water. Yield: 58% based on Cu. *Anal*. Calc. for $C_{62}H_{56}N_8O_{21}Cu_4S_2$ **1**: C, 47.47; H, 3.57; N, 7.15; S, 4.08. Found: C, 47.52; H, 3.48; N, 7.13; S, 4.12%. IR (KBr, cm^{-1}): 3407vs, 1603s, 1563m, 1522w, 1472m, 1414m, 1320m, 1221m, 1167m, 1131s, 1146s, 1020s, 849s, 722vs, 604m, 479w.

2.2.2. $Cu_4(OH)_2(ssal)_2(bipy)_4 \cdot 2H_2O$ (*2*)

The hydrothermal procedure for the synthesis of complex **2** is similar to that for **1** except for the replacement of phen with 2,2-bipy (0.082 g, 0.5 mmol). Yield: 82% based on Cu. *Anal*. Calc. for $C_{54}H_{44}N_8O_{16}Cu_4S_2$ **2**: C, 46.98; H, 3.19; N, 8.12; S, 4.64. Found: C, 46.85; H, 3.02; N, 8.09; S, 4.58%. IR (KBr, cm^{-1}): 3444m, 1602s, 1562m, 1470m, 1413w, 1341w, 1253w, 1211m, 1186m, 1150m, 1030s 771m, 604m, 470w.

2.2.3. Cd(Hssal)(bipy) (*3*)

A mixture of $3CdSO_4 \cdot 8H_2O$ (0.403 g, 0.5 mmol), 5-sulfosalicylic acid (0.132 g, 0.5 mmol), 2,2′-bipy (0.081 g, 0.5 mmol), KOH (0.08 g, 1.4 mmol) and water (15 ml) was stirred for 30 min at room temperature, transferred to and sealed in a 25 ml Teflon-lined stainless steel reactor, and then heated at 150 °C for 72 h. Upon cooling to room temperature, the light red crystals that were obtained were filtered and washed with water. Yield: 58% based on Cd. *Anal.* Calc. for $C_{17}H_{12}N_2O_6CdS$ **3**: C, 42.08; H, 2.48; N, 4.95; S, 6.60. Found: C, 41.94; H, 2.52; N, 4.87; S, 6.63%. IR (KBr, cm^{-1}): 3112m, 1626w, 1596m, 1559m, 1478m, 1440m, 1254m, 1158m, 1127s, 1017s, 769m, 676m, 602m.

2.2.4. $Cd(HL)_2(phen)_2$ (*4*)

A mixture of $3CdSO_4 \cdot 8H_2O$ (0.407 g, 0.5 mmol), 5-sulfosalicylic acid (0.132 g, 0.5 mmol), phen (0.108 g, 0.5 mmol), KOH (0.071 g, 1.3 mmol) and water (15 ml) was stirred for 30 min at room temperature, transferred to and sealed in a 25 ml Teflon-lined stainless steel reactor, and then heated at 150 °C for 72 h. Upon cooling to room temperature, a colorless solution and a spot of white precipitate were obtained. The solution was filtered and the filtrate was allowed to stand at room temperature. After slow evaporation over several days, red block single crystals were obtained. Yield: 62% based on Cd. *Anal*. Calc. for $C_{36}H_{26}N_4O_8CdS_2$ **4**: C, 52.74; H, 3.17; N, 6.84; S, 7.81. Found: C, 52.67; H, 3.23; N, 6.79; S, 7.83%. IR (KBr, cm^{-1}): 3168m, 1586m, 1506m, 1424m, 1237s, 1156s, 1122s, 1031s, 844s, 728s, 566m, 451w.

2.2.5. $Cr(ssal)(bipy)_2(H_2O)_2 \cdot 2H_2O$ (*5*)

A mixture of $Cr_2(SO_4)_3 \cdot 6H_2O$ (0.255 g, 0.5 mmol), 5-sulfosalicylic acid (0.134 g, 0.5 mmol), 2,2′-bipy (0.082 g, 0.5 mmol), KOH (0.051 g, 0.9 mmol) and water (15 ml) was stirred for 30 min at room temperature, transferred to and sealed in a 25 ml Teflon-lined stainless steel reactor, and then heated at 150 °C for 72 h. Upon cooling to room temperature, the green crystals that were obtained were filtered and washed with water. Yield: 5% based on Cr. *Anal*. Calc. for $C_{17}H_{19}N_2O_{10}CrS$ **5**: C, 41.18; H, 3.84;

N, 5.65; S, 6.46. Found: C, 41.11; H, 3.90; N, 5.57%. IR (KBr, cm^{-1}): 3446s, 1608s, 1571m, 1447m, 1472m, 1150s, 1031s, 763m, 602m.

2.2.6. Cr(ssal)(phen)$_2$ (6)

A mixture of $Cr_2(SO_4)_3 \cdot 6H_2O$ (0.253 g, 0.5 mmol), 5-sulfosalicylic acid (0.136 g, 0.5 mmol), phen (0.106 g, 0.5 mmol), KOH (0.062 g, 1.1 mmol) and water (15 ml) was stirred for 30 min at room temperature, transferred to and sealed in a 25 ml Teflon-lined stainless steel reactor, and then heated at 150 °C for 72 h. Upon cooling to room temperature, a red solution was obtained, which was filtered and the filtrate was allowed to stand at room temperature. After slow evaporation over several days, red block single crystals were obtained. Yield: 35% based on Cr. *Anal*. Calc. for $C_{31}H_{19}N_4O_6CrS$ **6**: C, 59.28; H, 3.03; N, 8.92; S, 5.10. Found: C, 59.35; H, 2.84; N, 8.97; S, 5.18%. IR (KBr, cm^{-1}): 3078vw, 1608s, 1574m, 1517m, 1469s, 1426s, 1311m, 1167s, 1033s, 845m, 721m, 601m, 451m.

2.2.7. Mn(Hssal)(bipy)$_2$(H$_2$O) · 2H$_2$O (7)

The hydrothermal procedure for the synthesis of complex **7** is similar to that for **6** except for the replacement of $Cr_2(SO_4)_3 \cdot 6H_2O$ with $MnCl_2 \cdot 4H_2O$ (0.108 g, 0.5 mmol). The yellow solution was obtained, filtered, and the filtrate was allowed to stand at room temperature. After slow evaporation over several days, yellow block single crystals were obtained. Yield: 65% based on Mn. *Anal*. Calc. for $C_{27}H_{26}N_4O_9MnS$ **7**: C, 50.82; H, 4.08; N, 8.78; S, 5.02. Found: C, 50.65; H, 3.96; N, 8.97; S, 5.18%. IR (KBr, cm^{-1}): 3453s, 1592s, 1517m, 1469s, 1426m, 1311m, 1167vs, 1033s, 845m, 721s, 601m, 451m.

2.2.8. Zn(Hssal)(bipy)(H$_2$O)$_2$ (8)

The hydrothermal procedure for the synthesis of complex **8** is similar to that for **6** except for the replacement of $Cr_2(SO_4)_3 \cdot 6H_2O$ with $ZnCl_2$ (0.074 g, 0.5 mmol). A colorless solution and a spot of white deposition were obtained. The solution was filtered and the filtrate was allowed to stand at room temperature. After slow evaporation over several days, colorless block single crystals were obtained. Yield: 72% based on Zn. *Anal*. Calc. for $C_{17}H_{16}N_2O_8SZn$ **8**: C, 43.06; H, 3.38; N, 5.91; S, 6.75. Found: C, 44.12; H, 3.66; N, 5.97; S, 6.68%. IR (KBr, cm^{-1}): 3283s, 1584s, 1441s, 1153vs, 1053s, 672s, 567s.

2.3. X-ray diffraction data and crystal structure determination

The crystal structures were determined by a single-crystal X-ray diffraction experiment. The reflection data were collected on a Bruker SMART CCD area-detector diffractometer (Mo Kα radiation, graphite monochromator) at room temperature with the ω-scan mode. Empirical adsorption corrections were applied to all data using the SADABS

Table 1
The crystallographic data for complexes **1**–**6**

	1	2	3	4	5	6
Empirical formula	$C_{62}H_{56}Cu_4N_8O_{21}S_2$	$C_{54}H_{44}Cu_4N_8O_{16}S_2$	$C_{17}H_{12}CdN_2O_6S$	$C_{36}H_{26}CdN_4O_8S_2$	$C_{17}H_{19}CrN_2O_{10}S$	$C_{31}H_{19}CrN_4O_6S$
Formula weight	1567.43	1379.25	484.75	819.16	495.40	627.57
Crystal system	monoclinic	monoclinic	triclinic	monoclinic	monoclinic	monoclinic
Space group	*P*2(1)/*c*	*P*2(1)/*c*	$P\bar{1}$	*C*2/*c*	*P*2(1)/*c*	*C*2/*c*
a (Å)	10.839(2)	10.919(1)	8.553(2)	20.307(6)	10.102(2)	31.602(4)
b (Å)	14.459(3)	12.405(7)	9.809(2)	13.753(9)	14.882(4)	10.265(2)
c (Å)	19.674(4)	20.239(3)	10.562(3)	14.296(9)	14.206(3)	16.536(2)
α (°)	90	90	93.984(4)	90	90	90
β (°)	102.575(4)	104.452(2)	103.786(4)	123.917(4)	110.669(3)	105.406(2)
γ (°)	90	90	104.416(4)	90	90	90
Volume	3010.3(1)	2654.0(6)	825.7(3)	3313.1(4)	1998.3(8)	5171.8(1)
Z	2	2	2	4	4	8
ρ_{calc} (g cm^{-3})	1.730	1.726	1.950	1.642	1.647	1.612
Absorption coefficient (mm^{-1})	1.553	1.741	1.489	0.847	0.737	0.581
θ Range (°)	1.76–26.08	1.94–26.09	2.00–26.10	1.91–26.06	2.05–26.11	1.34–26.04
Reflections collected	17220	15230	4660	9111	11286	14198
Unique reflections [R_{int}]	5911 [0.0777]	5232 [0.0518]	3178 [0.0212]	3276 [0.0137]	3932 [0.0477]	5101 [0.0409]
Completeness	99.1%	99.3%	97.0%	99.7%	98.8%	99.9%
Goodness-of-fit on F^2	0.998	1.024	1.032	1.060	1.040	1.023
R indexes [$I > 2\sigma(I)$][a]	$R_1 = 0.0533$, $wR_2 = 0.1023$	$R_1 = 0.0494$, $wR_2 = 0.1084$	$R_1 = 0.0403$, $wR_2 = 0.0872$	$R_1 = 0.0423$, $wR_2 = 0.1106$	$R_1 = 0.0697$, $wR_2 = 0.1646$	$R_1 = 0.0529$, $wR_2 = 0.1175$
R (all data)[a]	$R_1 = 0.1034$, $wR_2 = 0.1202$	$R_1 = 0.0724$, $wR_2 = 0.1203$	$R_1 = 0.0512$, $wR_2 = 0.0921$	$R_1 = 0.0438$, $wR_2 = 0.1121$	$R_1 = 0.1054$, $wR_2 = 0.1841$	$R_1 = 0.0797$, $wR_2 = 0.1318$

[a] $R_1 = \sum||F_o| - |F_c||/\sum|F_o|$; $wR_2 = [\sum w(F_o^2 - F_c^2)_2/\sum w(F_o^2)^2]^{1/2}$.

Table 2
Selected bond lengths (Å) and angles (°) for complexes **1-6**

Compound **1**			
Cu(1)–O(7)	1.947(3)	O(7)–Cu(1)–N(3)	161.3(4)
Cu(1)–O(7)#1	1.947(4)	O(7)#1–Cu(1)–N(3)	99.1(4)
Cu(1)–N(4)	2.009(4)	N(4)–Cu(1)–N(3)	82.0(2)
Cu(1)–N(3)	2.012(4)	O(7)–Cu(1)–O(3)	97.8(9)
Cu(1)–O(3)	2.297(3)	O(7)#1–Cu(1)–O(3)	85.0(1)
Cu(1)–Cu(1)#1	2.939(1)	N(4)–Cu(1)–O(3)	93.1(2)
Cu(2)–O(3)	1.882(3)	N(3)–Cu(1)–O(3)	100.8(1)
Cu(2)–O(1)	1.907(3)	O(3)–Cu(2)–O(1)	93.2(3)
Cu(2)–N(1)	2.005(4)	O(3)–Cu(2)–N(1)	171.1(9)
Cu(2)–N(2)	2.021(4)	O(1)–Cu(2)–N(1)	95.5(4)
O(7)–Cu(1)–O(7)#1	82.0(7)	O(3)–Cu(2)–N(2)	90.5(4)
O(7)–Cu(1)–N(4)	97.4(3)	O(1)–Cu(2)–N(2)	165.7(1)
O(7)#1–Cu(1)–N(4)	177.9(6)	N(1)–Cu(2)–N(2)	81.2(6)
Compound **2**			
Cu(1)–O(7)#2	1.952(3)	O(7)–Cu(1)–N(4)	159.7(2)
Cu(1)–O(7)	1.966(3)	N(3)–Cu(1)–N(4)	80.6(7)
Cu(1)–N(3)	1.994(3)	O(7)#1–Cu(1)–O(6)	83.7(5)
Cu(1)–N(4)	2.012(3)	O(7)–Cu(1)–O(6)	96.0(1)
Cu(1)–O(6)	2.221(3)	N(3)–Cu(1)–O(6)	96.4(5)
Cu(1)–Cu(1)#2	2.989(1)	N(4)–Cu(1)–O(6)	104.2(5)
Cu(2)–O(6)	1.908(3)	O(6)–Cu(2)–O(5)	91.8(1)
Cu(2)–O(5)	1.916(3)	O(6)–Cu(2)–N(2)	175.0(2)
Cu(2)–N(2)	1.984(3)	O(5)–Cu(2)–N(2)	93.2(1)
Cu(2)–N(1)	2.017(4)	O(6)–Cu(2)–N(1)	93.9(6)
Cu(2)–O(7)#2	2.311(3)	O(5)–Cu(2)–N(1)	158.1(4)
O(7)#1–Cu(1)–O(7)	80.5(8)	N(2)–Cu(2)–N(1)	81.3(2)
O(7)#1–Cu(1)–N(3)	179.2(7)	O(6)–Cu(2)–O(7)#2	82.2(8)
O(7)–Cu(1)–N(3)	98.7(1)	O(5)–Cu(2)–O(7)#2	102.4(7)
O(7)#1–Cu(1)–N(4)	100.0(1)	N(2)–Cu(2)–O(7)#2	96.9(1)
		N(1)–Cu(2)–O(7)#2	99.2(3)
Compound **3**			
Cd(1)–N(2)	2.305(3)	O(2)–Cd(1)–O(1)	54.8(3)
Cd(1)–O(2)	2.305(3)	O(6)–Cd(1)–O(1)	91.9(4)
Cd(1)–O(6)	2.318(3)	N(1)–Cd(1)–O(1)	86.2(5)
Cd(1)–N(1)	2.327(4)	N(2)–Cd(1)–O(4)	86.4(1)
Cd(1)–O(1)	2.452(3)	O(2)–Cd(1)–O(4)	82.2(6)
Cd(1)–O(4)	2.584(3)	O(6)–Cd(1)–O(4)	120.0(6)
Cd(1)–O(6)#3	2.619(3)	N(1)–Cd(1)–O(4)	80.0(3)
N(2)–Cd(1)–O(2)	168.1(8)	O(1)–Cd(1)–O(4)	130.2(8)
N(2)–Cd(1)–O(6)	91.1(4)	N(2)–Cd(1)–O(6)#3	92.0(4)
O(2)–Cd(1)–O(6)	97.4(1)	O(2)–Cd(1)–O(6)#3	83.9(7)
N(2)–Cd(1)–N(1)	71.3(8)	O(6)–Cd(1)–O(6)#3	66.2(5)
O(2)–Cd(1)–N(1)	103.2(6)	N(1)–Cd(1)–O(6)#3	132.4(3)
O(6)–Cd(1)–N(1)	153.1(9)	O(1)–Cd(1)–O(6)#3	131.1(6)
N(2)–Cd(1)–O(1)	133.3(9)	O(4)–Cd(1)–O(6)#3	54.0(5)
Compound **4**			
Cd(1)–O(1)	2.236(3)	N(1)#4–Cd(1)–N(1)	163.7(5)
Cd(1)–N(1)	2.341(3)	O(1)–Cd(1)–N(2)#4	160.2(8)
Cd(1)–N(2)	2.346(3)	N(1)–Cd(1)–N(2)#4	71.4(7)
O(1)–Cd(1)–O(1)#4	88.4(3)	O(1)–Cd(1)–N(2)	92.8(9)
O(1)–Cd(1)–N(1)#4	102.6(9)	N(1)–Cd(1)–N(2)	97.0(4)
O(1)–Cd(1)–N(1)	89.0(5)	N(2)#4–Cd(1)–N(2)	92.4(8)
Compound **5**			
Cr(1)–O(3)	1.881(3)	O(2)–Cr(1)–O(4W)	91.4(2)
Cr(1)–O(2)	1.918(3)	O(3W)–Cr(1)–O(4W)	179.4(1)
Cr(1)–O(3W)	1.997(4)	O(3)–Cr(1)–N(1)	93.8(9)
Cr(1)–O(4W)	1.997(4)	O(2)–Cr(1)–N(1)	172.7(5)
Cr(1)–N(1)	2.062(4)	O(3W)–Cr(1)–N(1)	90.2(9)
Cr(1)–N(2)	2.067(4)	O(4W)–Cr(1)–N(1)	90.1(1)
O(3)–Cr(1)–O(2)	93.2(6)	O(3)–Cr(1)–N(2)	172.0(3)
O(3)–Cr(1)–O(3W)	91.4(6)	O(2)–Cr(1)–N(2)	94.7(4)
O(2)–Cr(1)–O(3W)	88.1(6)	O(3W)–Cr(1)–N(2)	89.0(9)
O(3)–Cr(1)–O(4W)	89.0(1)	O(4W)–Cr(1)–N(2)	90.5(4)
		N(1)–Cr(1)–N(2)	78.1(7)
Complex **6**			
Cr(1)–O(3)	1.886(2)	O(1)–Cr(1)–N(1)	93.8(1)
Cr(1)–O(1)	1.912(2)	N(3)–Cr(1)–N(1)	169.8(9)
Cr(1)–N(3)	2.061(3)	O(3)–Cr(1)–N(4)	87.6(3)
Cr(1)–N(1)	2.064(3)	O(1)–Cr(1)–N(4)	173.1(2)
Cr(1)–N(4)	2.077(3)	N(3)–Cr(1)–N(4)	79.7(5)
Cr(1)–N(2)	2.091(3)	N(1)–Cr(1)–N(4)	93.1(1)
O(3)–Cr(1)–O(1)	91.8(4)	O(3)–Cr(1)–N(2)	173.6(5)
O(3)–Cr(1)–N(3)	92.5(3)	O(1)–Cr(1)–N(2)	90.5(6)
O(1)–Cr(1)–N(3)	93.4(3)	N(3)–Cr(1)–N(2)	93.2(3)
O(3)–Cr(1)–N(1)	94.3(3)	N(1)–Cr(1)–N(2)	79.6(4)
		N(4)–Cr(1)–N(2)	90.7(3)

#1 $-x+1$, $-y$, $-z+2$; #2 $-x+1$, $-y$, $-z$; #3 $-x+1$, $-y$, $-z+1$; #4 $-x+1$, y, $-z+1/2$.

Table 3
Geometrical parameters of hydrogen bonds in complexes **1**–**6**

D–H···A	d(D–H)	d(H···A)	d(D···A)	∠(DHA)
Compound **1**				
O7–H9···O4(a)	0.69	2.28	2.98	176.24
O1w···O4w(b)			2.89	
O1w···O4w(c)			2.89	
O2w···O4(d)			3.13	
O2w···O3			2.79	
O3w–H3wA···O2(e)	0.85	1.96	2.76	155.82
O3w–H3wB···O4w(f)	0.85	2.10	2.90	156.84
O4w–H4wB···O1w(g)	0.85	2.25	2.89	131.71
O4w–H4wA···O6	0.85	1.99	2.79	155.77
Compound **2**				
O1w···O1(h)			2.87	
O1w···O4(i)			2.95	
O7–H20···O4(j)	0.83	2.02	2.85	172.30
Compound **3**				
C7–H12···O5(k)	0.96	2.44	3.41	174.72
C4–H1···O5(k)	0.97	2.43	3.39	175.51
Compound **4**				
O4–H13···O3(l)	0.91	1.93	2.71	141.49
Compound **5**				
O1w–H1wA···O4(m)	0.87	2.28	3.00	140.36
O1w–H1wB···O1(n)	0.85	1.95	2.80	168.89
O2w–H2wA···O1(o)	0.86	1.94	2.79	167.20
O2w–H2wB···O5(p)	0.85	1.83	2.67	176.29
O3w–H3wA···O2w(q)	0.84	1.78	2.61	172.77
O3w–H3wB···O4(r)	0.85	1.97	2.72	146.25
O4w–H4wA···O1w(s)	0.84	1.78	2.61	172.12
O4w–H4wB···O6(t)	0.82	1.88	2.67	162.98
Compound **6**				
C10–H4···O5(u)	0.95	2.30	3.11	141.26
C22–H9···O4(v)	0.94	2.35	3.07	132.46

Symmetry code: (a) $-x+1$, $y-1/2$, $-z+3/2$; (b) $1-x$, $1-y$, $1-z$; (c) $-1+x$, y, $-1+z$; (d) x, $0.5-y$, $-0.5+z$; (e) x, y, $z-1$; (f) $-x+2$, $-y+1$, $-z+1$; (g) $x+1$, y, $z+1$; (h) $-1+x$, y, z; (i) $1-x$, $1-y$, $-z$; (j) $-x+1$, $y+1/2$, $-z+3/2$; (k) $1-x$, $-y$, $-$;z; (l) x, $-y$, $z+1/2$; (m) $-x+1$, $-y+1$, $-z+1$; (n) $x+1$, $-y+1/2$, $z+1/2$; (o) $x+1$, y, z; (p) $-x+1$, $-y+1$, $-z$; (q) $-x+1$, $y-1/2$, $-z+1/2$; (r) $-x$, $y-1/2$, $-z+1/2$ (s) $-x+1$, $y-1/2$, $-z+1/2$; (t) $-x+1$, $y-1/2$, $-z+1/2$; (u) x, $2-y$, $-0.5+z$; (v) x, $1-y$, $-0.5+z$.

program. The structures were solved by direct methods and refined by full-matrix least squares on F^2 using SHELXTL97 software [11]. Non-hydrogen atoms were refined anisotropically. The hydrogen atoms were located from difference maps and refined with isotropic temperature factors in complexes **1**–**6**. All calculations were carried out using SHELXTL97 [11] and PLATON99 [12]. The crystallographic data and pertinent information are summarized in Table 1, and any additional refinement information is given below.

Complex **1** O1w showed disorder over two positions and was refined at 0.50 and 0.50 occupancy for each position. The hydrogen atoms of O1 w, O2w and O3w were not located from difference Fourier maps, and the O–H distances of O4w were refined with a DFIX restraint of 0.85 Å.

Complex **2** Hydrogen atoms of O1w were not located from difference Fourier maps.

Complex **5** O2 and O3 atoms of the sulfonate group both showed disorder over two positions and were refined at 0.50 and 0.50 occupancy, and 0.41 and 0.59 occupancy, respectively.

Selected bond lengths and angles for complexes **1**–**6** are summarized in Table 2. Geometrical parameters of the hydrogen bonds in complexes **1**–**6** are summarized in Table 3.

3. Results and discussion

3.1. Synthesis

5-Sulfosalicylic acid and bipyridyl-like mixed ligands were reacted in aqueous medium with different metal salts ($Cr_2(SO_4)_3 \cdot 6H_2O$, $MnCl_2 \cdot 4H_2O$, $CuSO_4 \cdot 5H_2O$, $ZnCl_2$, $3CdSO_4 \cdot 8H_2O$) in a molar ratio of 1:1:1 at different pH levels ranging from 5 to10 in an attempt to investigate the reactivity. The reactions were carried out in a 25 ml Teflon-lined stainless steel reactor at 150 °C for 72 h. We obtained compounds **1**–**8** (Scheme 1) at different pH values. Coordination complexes of Cr(III), Cu(II) and Cd(II) were obtained under weakly acidic, neutral and weakly basic conditions, respectively. Complexes **7** and **8** were easily obtained for the wider pH range 5–8. It is worth noting that complexes **1**, **2**, **3** and **5** were all directly obtained through the hydrothermal method, however, complexes **4**, **6**, **7** and **8** were synthesized through evaporation of the filtrate after the hydrothermal reaction. We tried to synthesize complexes **4**, **6**, **7** and **8** at room temperature, but failed. This demonstrates that complexes **4**, **6**, **7** and **8** were synthesized under hydrothermal conditions.

3.2. Crystal structures of the complexes

3.2.1. Structure description of $Cu_4(OH)_2(ssal)_2(phen)_4 \cdot 7H_2O$ (**1**)

X-ray single crystal diffraction reveals that compound **1** possesses a centrosymmetric Cu_4O_4 core based on a stepped topology (Fig. 1) [13]. The Cu_4O_4 core is composed of two crystallographically independent Cu (II) atoms [namely, Cu1 and Cu2]. Cu1 and Cu2 both possess the configuration of a distorted square pyramid, however, there are two sets of coordination environments around the copper atoms. Cu1 is located in a plane consisting of two nitrogen atoms (N3 and N4) from a chelating phen molecule and two hydroxides (O7 and O7#1), and the axial position is occupied by the phenolato oxygen atom (O3). For Cu2, the plane is composed of two nitrogen atoms (N1 and N2) from the phen molecule, one carboxylate oxygen (O1) and one phenolato oxygen atom (O3), and the corresponding axial position is taken by one hydroxide ion (O7#1). Cu1 and Cu2 atoms, with two symmetry-related copper centres, are connected into a Cu_4O_4 core by two μ_3-hydroxo groups and two phenolato oxygen atoms. The Cu_4O_4 core consists of a stepped structure in which three Cu_2O_2 planes are formed by Cu2 Cu1 O3 O7#1 I, Cu1 Cu1#1 O7 O7#1 II and Cu2#1 Cu1#1 O3#1 O7 III. Planes I and III, with a maximum deviation of 0.1308 Å from their least-squares planes, are parallel to each other, but both have the same bihedral angle of 103° with plane II. In the Cu_4O_4 core, we observed that the four Cu atoms form a flat rhomboid with sides Cu1···Cu2 and Cu1#1···Cu2 of lengths 3.18 and 3.59 Å, respectively, a short diagonal (Cu1···Cu1#1) of 2.94 Å and a long diagonal (Cu2···Cu2#1) of 6.10 Å. Offset π–π interactions between phen molecules with a face-to-face distance of 3.43 Å and offset angle of 28.74° stabilize the tetranuclear complex. To the best of our knowledge, only one copper complex constructed from mixed organic ligands with a stepped topology has previously been reported [13a].

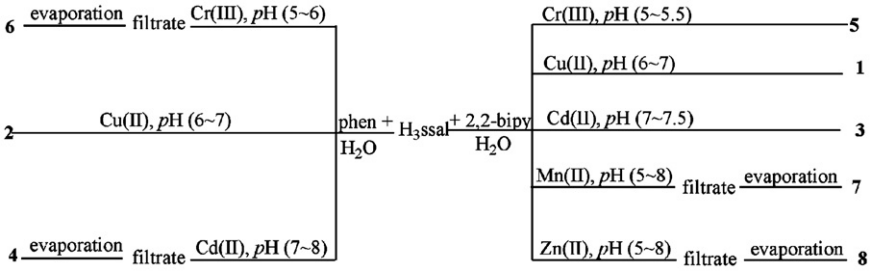

Scheme 1. The reactions to prepare complexes **1**–**8**.

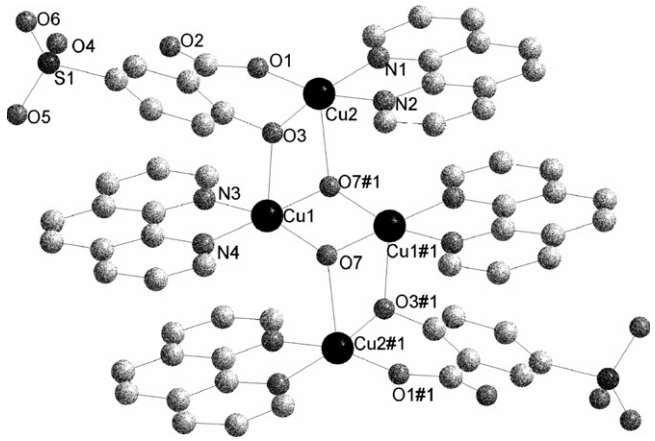

Fig. 1. The molecular structure of complex **1**.

Each $Cu_4(OH)_2(ssal)_2(phen)_4$ molecule is linked to four neighboring tetrameric units to form a 2D supramolecular layer (S-Fig. 1) of rhombic windows (with dimensions of 6.05×13.44 Å) through hydrogen bonding between μ_3-hydroxo groups (O7) and the uncoordinated sulfonate oxygen atoms (O4). The 2D layers are connected into a 3D supramolecular network by water heptamers (Fig. 2), the geometrical parameters of the hydrogen bonds are given in Table 3. In addition to hydrogen bonding, inter-layer contacts are strengthened by intermolecular π–π interactions between adjacent $Cu_4(OH)_2(ssal)_2(phen)_4$ units (offset π–π interaction between phen molecules with a face-to-face distance of 3.47 Å and offset angle 36.53°). Interestingly, the water heptamers and sulfonate anions are interconnected into a 2D supramolecular layer with very large rhombic windows (with dimensions of 12.57×17.77 Å) through hydrogen bonding (Fig. 3). The tetranuclear Cu (II) units are right inside the large rhombic windows between the 2D layers (S-Fig. 2).

3.2.2. Structure description of $Cu_4(OH)_2(ssal)_2(bipy)_4 \cdot 2H_2O$ (**2**)

Complexes **1** and **2** have the same space group, $P2_1/c$. The molecular structures of complexes **1** and **2** show some similarities as follows: (a) Both possess the centrosymmetric Cu_4O_4 (S-Fig. 3) core based on a stepped topology. (b) The central copper atoms in both complexes have the same coordination geometry, and the bond lengths and angles, as shown in Table 2, are also similar. (c) Both possess similar 2D supramolecular layers based on tetranuclear Cu (II) units. However, the replacement of phen by bipy, a chelating aromatic ligand of a smaller size, leads to some subtle differences. One difference worth noticing between the crystal structures of **1** and **2** concerns the numbers of water molecules in their asymmetric units: 3.5 water molecules for **1** and one water molecule for **2**. This results in the formation of a 3D supramolecular network (Fig. 4) for compound **2** differing from that of compound **1**. In compound **2**, the 2D layers are connected into a 3D supramolecular network through O1w with symmetry-related layers and π–π interactions between adjacent $Cu_4(OH)_2(ssal)_2(bipy)_4$ units (offset π–π interactions between 2,2′-bipy molecules with a face-to-face distance of 3.54 Å and offset angle of 24.71°).

3.2.3. Structure description of Cd(Hssal)(bipy) (**3**)

The crystal analysis of complex **3** reveals that it is a one-dimensional ladder coordination polymer containing Cd_2O_8 (2,2′-bipy)$_2$ units (Fig. 5a) with Hssal as the bridge ligands. The asymmetric unit of complex **3** consists of one Cd atom, one Hssal anion and one 2,2′-bipy ligand. The Cd center adopts a distorted capped-octahedral conformation (Fig. 5b) in which the basal plane is formed by two nitrogen atoms (N1 and N2) from a chelating 2,2′-bipy ligand, a carboxylate oxygen atom (O2) and a sulfonate oxygen atom (O6) from two different Hssal anions. The axial positions are taken by a carboxylate oxygen atom

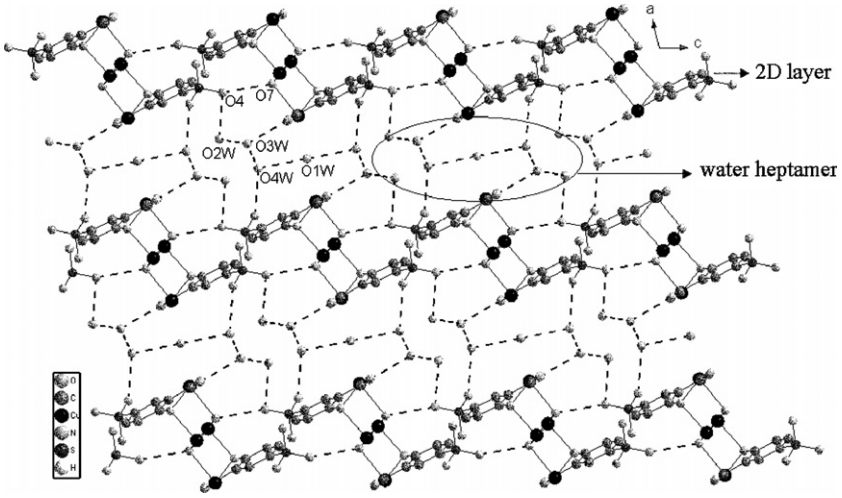

Fig. 2. Perspective view of the 3D supramolecular network of complex **1**, phen ligands and H atoms were removed for clarity.

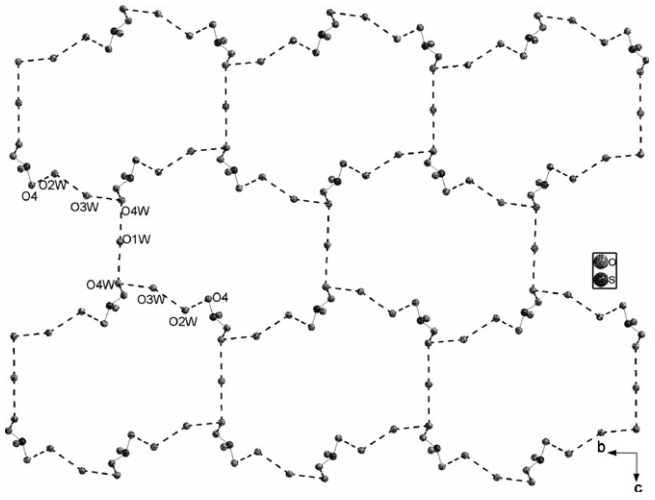

Fig. 3. 2D supramolecular layer consisting of hydrogen bonded water heptamers and sulfonate anions in complex **1**.

(O1) and a sulfonate oxygen atom (O6#3). The sulfonate oxygen atom (O4) occupies the capped position. Each pair of Cd ions is bridged by a sulfonate oxygen atom (O6) with symmetry-related partner (O6#3) to form a Cd_2O_8 (2,2′-bipy)$_2$ unit. These dimeric Cd_2 units, featuring a 1D ladder (Fig. 6a) along the crystallographic*a* axis, are interconnected by Hssal^{2-} anions. Each Hssal^{2-} anion connects three Cd (II) atoms (Fig. 6b) with the carboxylic group and sulfonate group, adopting $\mu_1 - \eta^1{:}\eta^1$-chelating and $\mu_2 - \eta^0{:}\eta^1{:}\eta^2$-bridging/chelating coordination modes [14]. As far as we know, this kind of new coordination mode of the Hssal^{2-} group has not been reported previously. The adjacent chains are further aggregated into a 2D sheet (S-Fig. 4) through π–π interactions between phen ligands, with a face-to-face distance of 3.47 Å and offset angle 36.52°, chelating C–H···O hydrogen bonding (C4···O5 = 3.39, C7···O5 = 3.41 Å) and C–H···π interactions between C8 and H5 from 2,2′-bipy ligands and Hssal^{2-} rings containing C16 (S-Fig. 5, H5···π = 2.72 and C8···π = 3.59 Å).

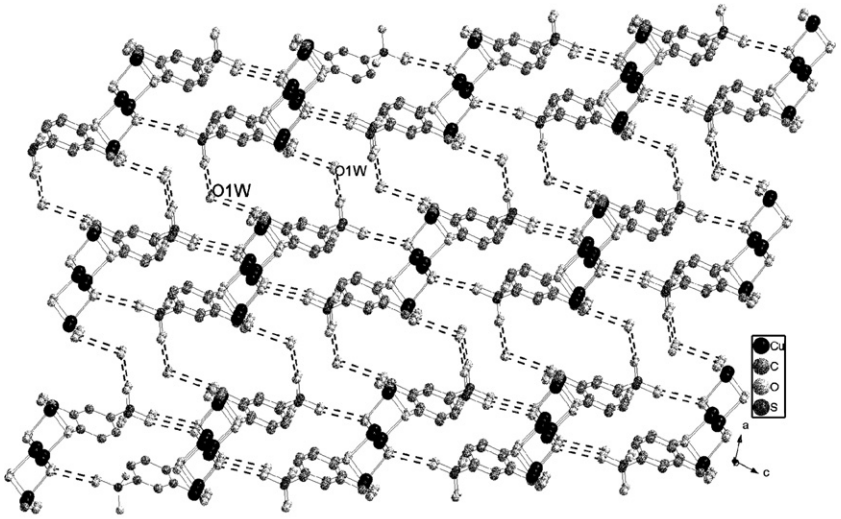

Fig. 4. Perspective view of the 3D supramolecular network of complex **2**, 2,2-bipy ligands were removed for clarity.

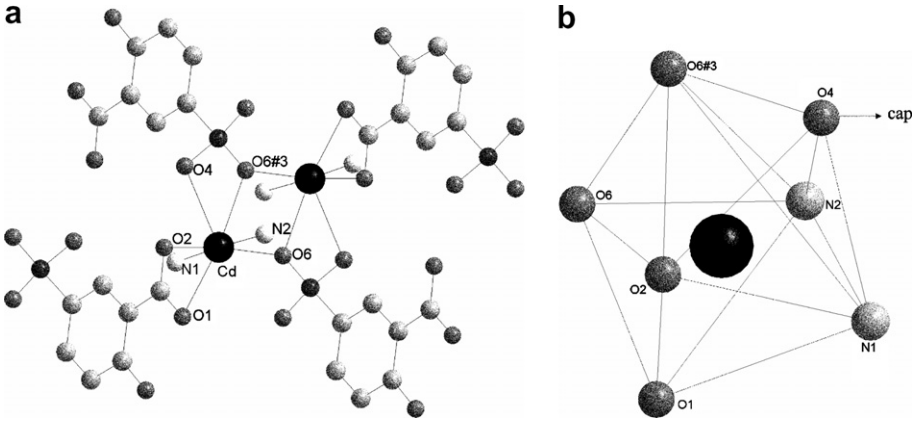

Fig. 5. (a) Perspective view of a dimeric Cd unit in complex **3**, the C atoms of 2,2′-bipy are omitted for clarity. (b) A distorted capped-octahedral conformation of the Cd (II) ion.

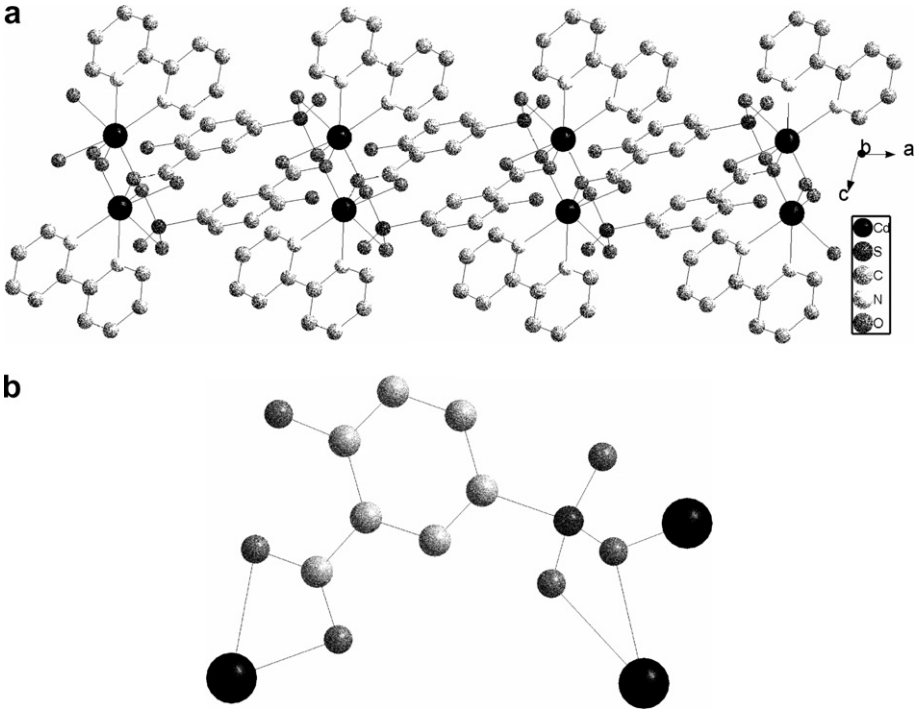

Fig. 6. (a) A 1D ladder constructed by dimeric $Cd_2O_8N_4$ units along the *a*-axis. (b) The coordination mode of the $Hssal^{2-}$ ligand in complex **3**.

3.2.4. Structure description of $Cd(HL)_2(phen)_2$ (**4**)

The crystal analysis of complex **4** reveals that it is a mononuclear complex consisting of one Cd (II) ion, two phen molecules and two *p*-hydroxybenzenesulfonic acid anions. The Cd (II) center exhibits a distorted octahedral surrounding (Fig. 7), in which the basal plane is formed by three nitrogen atoms (N1, N1#4 and N2) from two symmetry-related phen molecules and one sulfonate oxygen atom (O1#4). The axial positions are occupied by a nitrogen atom (N1#4) from a phen molecule and a sulfonate oxygen atom (O1). The π–π interactions between the aromatic rings of the different ligands are favorable to stabilize complex **4**. The closest centroid separation is 3.76 Å from the *p*-hydroxybenzenesulfonic ligand to the C_6 ring of the phen ligand, with an offset angle of 19.85°. Interestingly, the $Cd(L)_2(phen)_2$ molecules are connected into 1D supramolecular double chains (S-Fig. 6), sharing $Cd(phen)_2$ units by O–H···O hydrogen bonding (O4···O3 = 2.71 Å) along the crystallographic *c*-axis. The adjacent double chains are further aggregated into a 3D supramolecular network (Fig. 8) through π–π interactions between phen ligands (the closest centroid separation is 3.679 Å between C_6 rings with an offset angle of 16.31°) and C–H···O hydrogen bonding (C18···O2 = 3.20 Å).

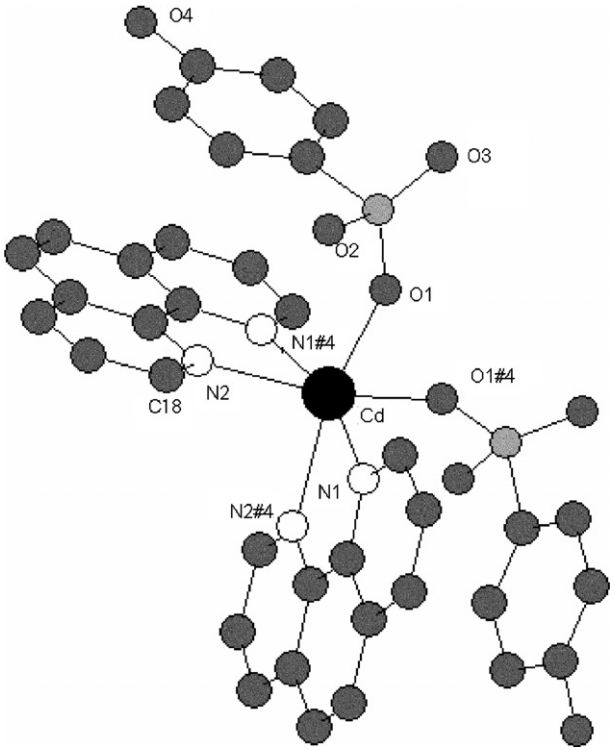

Fig. 7. The molecular structure of complex **4**.

3.2.5. Structure description of $Cr(ssal)(bipy)(H_2O)_2 \cdot 2H_2O$ (**5**)

X-ray single crystal diffraction reveals that the asymmetric unit of **5** contains one Cr(III) ion, one ssal anion, one 2,2′-bipy molecule, two coordinated water and two lattice water molecules. The Cr(III) center exhibits a distorted octahedral surrounding (Fig. 9), in which the basal plane is formed by two nitrogen atoms from a chelating 2,2′-bipy ligand (N1 and N2) and one carboxylate oxygen (O2) and one phenolic oxygen (O3) from a ssal ligand.

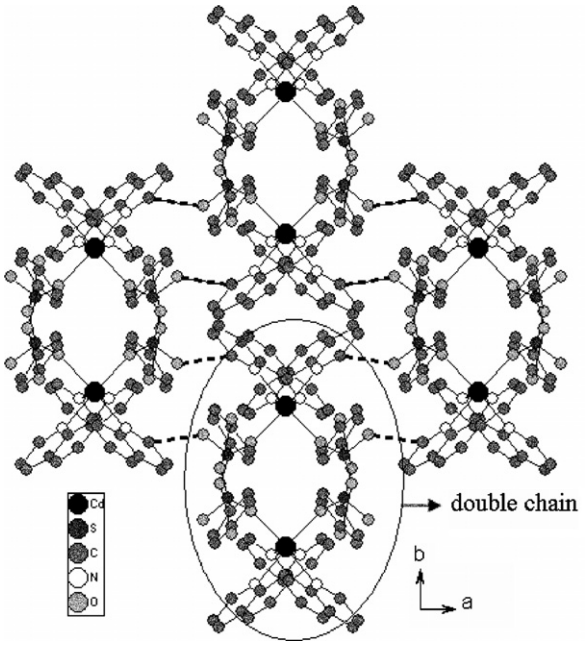

Fig. 8. The 3D supramolecular network in complex **4**.

The axial positions are occupied by O3w and O4w. Each $Cr(ssal)(bipy)_2(H_2O)_2$ unit is hydrogen bonded to two other units to form a 1D supramolecular helical chain (Fig. 9) resulting from O–H···O hydrogen bonds involving O3w, O2w, O1, O1w and O4. Within the chain, the π–π interactions between the aromatic rings of the different ligands may stabilize the polymeric supramolecular chain. The closest centroid separation is 4.01 Å from the $ssal^{3-}$ ligand to the C_5N ring (containing the N2 atom) of the 2,2′-bipy ligand with an offset angle of 26.09°. The 1D chains are further linked into a 2D layer (Fig. 10) through O–H···O hydrogen bonding (O2w···O5, O1w···O4w), the geometrical parameters of the hydrogen bonds of compound **5** are collected in Table 3. The most remarkable feature of this 2D layer is that there exist a supramolecular ring (S-Fig. 7) consisting of four coordinated water molecules (O3w and O4w), six lattice water molecules (O1w and O2w), three $ssal^{3-}$ anions and three Cr^{3+} ions, formed through covalent bonds and hydrogen bonds. Only the 2,2′-bipy molecules occupy the supramolecular rings, preventing interpenetration. Finally, the 2D layers are hydrogen bonded through O4wB-H4wB···O6 to afford a 3D supramolecular network (S-Fig. 8). Compared with some active transition metals (Zn, Cd, Cu, etc.), coordination complexes of Cr are relatively fewer due to its inertness (slow polymerization and difficulty of substitution) [15,16]. To the best of our knowledge, complex **5** is the first example of a chromium 5-sulfosalicylate complex.

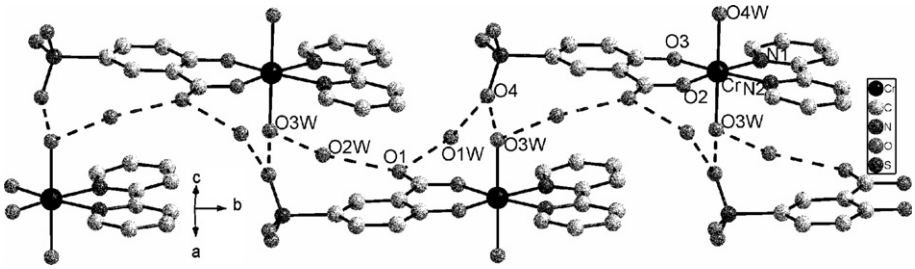

Fig. 9. 1D supramolecular helical chains consisting of $Cr(ssal)(bipy)_2(H_2O)_2$ units in complex **5**.

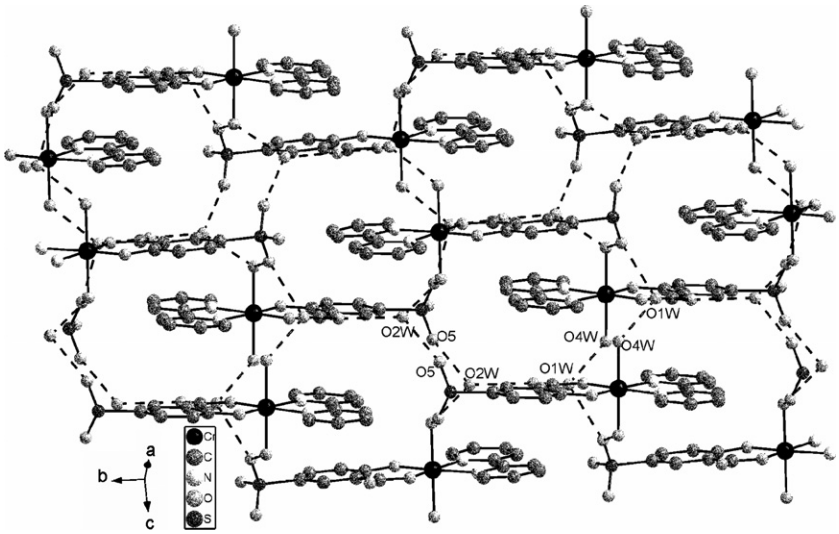

Fig. 10. Perspective view of the 2D supramolecular layer in complex **5**.

3.2.6. Structure description of Cr(ssal)(phen)$_2$ (6)

The asymmetric unit of **6** (Fig. 11) contains one Cr (III) ion, one ssal anion and two phen molecules. The Cr(III) center exhibits a distorted octahedral surrounding, in which the basal plane is formed by two nitrogen atoms from two different phen ligands (N2 and N4) and two bidentate chelating coordination oxygen atoms from one carboxylate oxygen (O1) and one phenolic oxygen (O3). The axial positions are occupied by N1 and N3 from two different phen ligands. Each Cr(ssal)(phen)$_2$ unit is hydrogen bonded to four other units to form a 2D puckered supramolecular layer (S-Fig. 9) through C–H···O (C10–H8···O5, C22–H9···O4). Moreover, O···π (S-Fig. 10, the distance of O5 to the C_5N ring containing the N3 atom is 3.10 Å) [17] and π···π interactions between the aromatic rings of different ligands (the closest centroid separation is 3.91 Å from the aryl of the ssal anion ligand to the C_6 ring of the phen ligand with an offset angle of 23.91°) stabilize the 2D puckered supramolecular layer. The 2D layers are held together into a 2D supramolecular double-layer through π···π interactions between phen ligands (the closest centroid separation is 3.79 Å between the C6 rings of phen ligands with an offset angle of 25.79°). The 2D double layers are further aggregated into a 3D supramolecular network (Fig. 12) through infinite π-stacking between the phen ligands in head-to-tail way (the closest centroid separation is 3.86 Å with an offset angle of 13.27°).

3.3. Magnetic studies of complexes 1–2

The variable temperature magnetic susceptibility of complexes **1** and **2** was measured at 1000 G in the temperature range 5–300 K. The magnetic behaviors of **1** are depicted in Fig. 13 in the forms of χ_M and μ_{eff} versus T plots (χ_M being the molar magnetic susceptibility). As the temperature is lowered, χ_M increases slowly until about 50 K, then it dramatically increases at lower temperatures. The data between 300 and 5 K can be fit to the Curie–Weiss expression, $\chi_M = C/(T-\theta)$, $[C = 0.125\, g^2 \sum S(S+1)]$, with the Curie constant $C = 1.71$ cm^3 K mol^{-1}, Weiss constant $\theta = 7.5$ K and $g = 2.14$. On the other hand, at room temperature the effective magnetic moment (μ_{eff}) equals 3.701 μ_B, which is slightly higher than the spin-only value of four

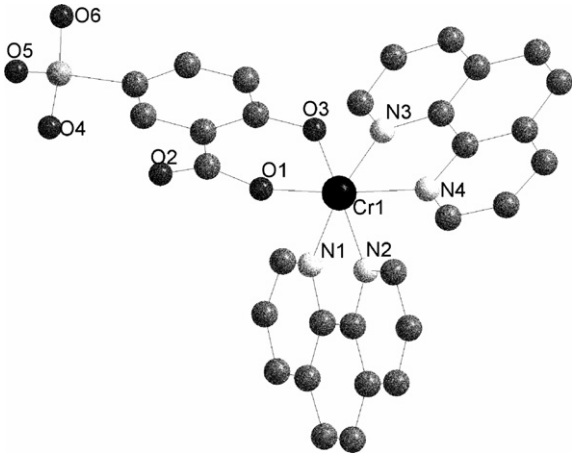

Fig. 11. The molecular structure of complex **6**. Hydrogen atoms are removed for clarity.

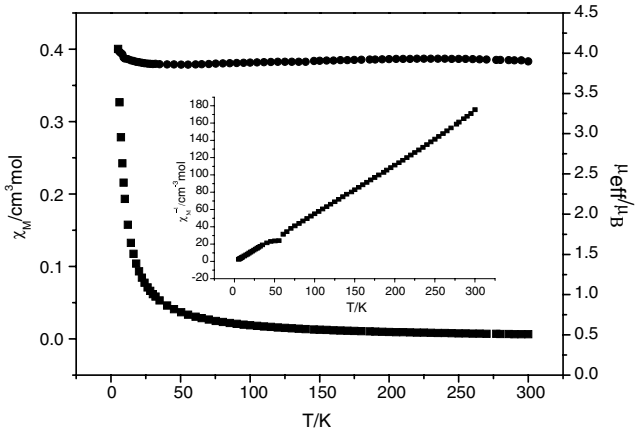

Fig. 13. Plots of χ_M and μ_{eff} vs. T for complex **1**. The inset is the plot of $1/\chi_M$ vs. T.

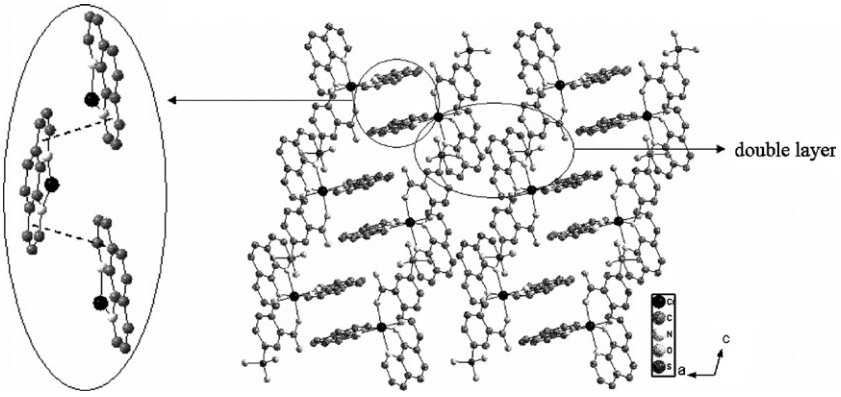

Fig. 12. The 3D representation of the packing arrangement for complex **6**. The insets show the existence of infinite π-stacking in a head-to-tail way. H atoms have been removed for clarity.

uncoupled copper (II) $S = 1/2$ ions (theoretical value for $g = 2$, $\mu_{eff} = 3.464\ \mu_B$). The μ_{eff} value increases gradually until 5 K, reaching a value of 4.037 μ_B. This feature is characteristic of the presence of significant ferromagnetic interactions between the copper (II) ions [13b,13f]. Moreover, the positive sign of the Weiss constant also indicates there exist ferromagnetic interactions between the Cu (II) centers.

The magnetic behavior of complex **2** is shown in Fig. 14 in the forms of χ_M and μ_{eff} versus T plots. As the temperature is lowered, χ_M increases slowly until about 38 K, then it dramatically increases at lower temperatures. The data between 300 and 38 K can be fit to the Curie–Weiss expression, $\chi_M = C/(T-\theta)$, $[C = 0.125\, g^2 S(S+1)]$, with the Curie constant $C = 0.784\ cm^3\ mol^{-1}$ K and Weiss constant $\theta = -0.401$ K. The effective magnetic moment (μ_{eff}) in **2** decreases slowly from 3.43 μ_B at 300 K to 3.21 μ_B at 55 K, and then falls rapidly, reaching 2.46 μ_B at 5 K. At room temperature the effective magnetic moment (μ_{eff}) equals 3.43 μ_B, which is slightly lower than the spin-only value of four uncoupled copper (II) $S = 1/2$ ions (theoretical value for $g = 2$, $\mu_{eff} = 3.46\ \mu_B$). These features indicate that there exist anti-ferromagnetic interactions amongst the Cu (II) centers [13e]. The difference in the magnetic properties of complexes **1** and **2** is possibly the result of the different intermolecular contacts.

3.4. Fluorescent properties of complexes 3–4

The solid-state fluorescent spectra of complexes **3** and **4** are depicted in Figs. 15 and 16, respectively. In order to understand the nature of the emission bands of complex **3** and **4**, we also investigated the luminescence of the free 2, 2-bipy, phen · H_2O and H_3ssal · $2H_2O$ ligands in the solid state at room temperature. The emission bands for free phen · H_2O are at 365, 381, 403 and 437 nm ($\lambda_{exc.} = 344$ nm), which may be attributed to the $\pi^* \rightarrow \pi$ transition (S-Fig. 11). Similar to free phen · H_2O, the emission bands for the free 2, 2-bipy ligand, at 390, 413 and 438 nm ($\lambda_{exc.} = 352$ nm), are also attributed to the $\pi^* \rightarrow \pi$ transition (S-Fig. 12). However, the emission bands for free H_3ssal · $2H_2O$ are mainly located at about 387 nm with a shoulder peak at 440 nm (H_3ssal · $2H_2O$: $\lambda_{exc.} = 335$ nm) and are attributed to $\pi^* \rightarrow n$ transitions (S-Fig. 13). Complex **3** exhibits intense green photoluminescence with an emission maximum at ca. 520 nm upon excitation at 347 nm (Fig. 15). Compared with the emission spectra of the free 2, 2-bipy and H_3ssal · $2H_2O$ ligands, the band at 520 nm for **3** might be assigned to the emission of a ligand-to-metal charge transfer (LMCT), similar to reported Cd complexes [18]. Complex **4** displays intense blue photoluminescence with an emission maximum at ca. 440 nm upon excitation at 329 nm (Fig. 16), compared with the emission spectra of the free phen · H_2O and H_3ssal · $2H_2O$ ligands, the band at 440 nm for **4** is neither LMCT (ligand-to-metal charge transfer) nor MLCT (metal-to-ligand charge transfer) in nature, and tentatively might be assigned to an intraligand fluorescent emission [19,20].

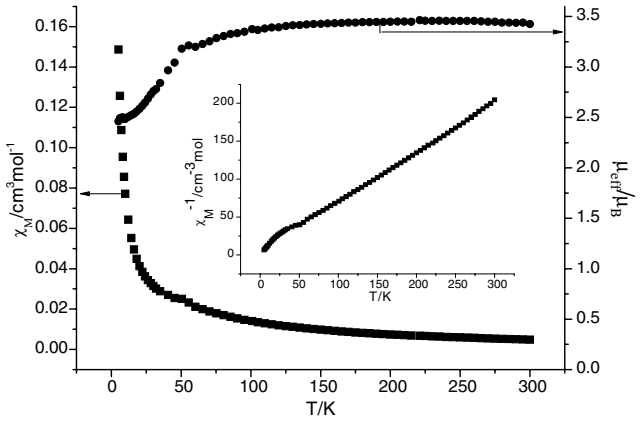

Fig. 14. plots of χ_M and μ_{eff} vs. T for complex **2**. The inset is the plot of $1/\chi_M$ vs. T.

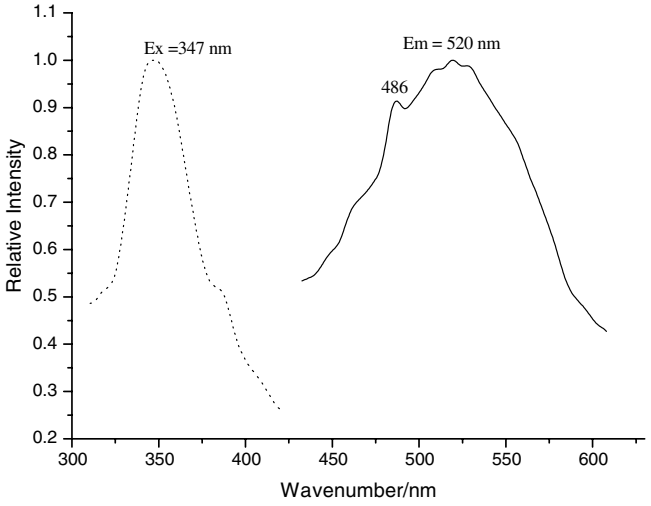

Fig. 15. Solid-state excitation fluorescent (dashed line) and emission (full line) spectra of complex **3** at room temperature.

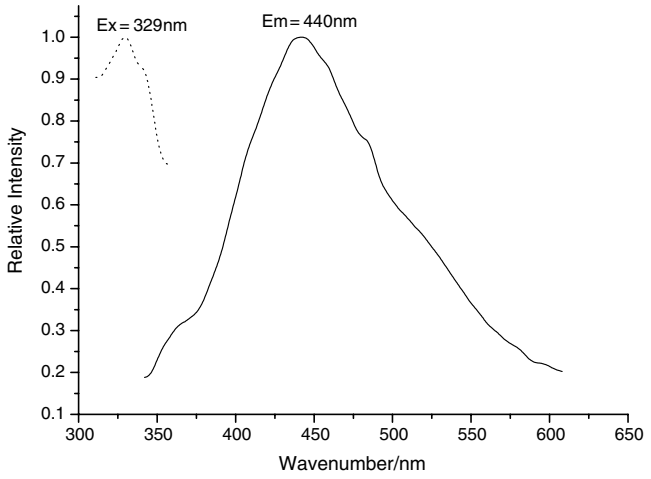

Fig. 16. Solid-state excitation fluorescent (dashed line) and emission (full line) spectra of complex **4** at room temperature.

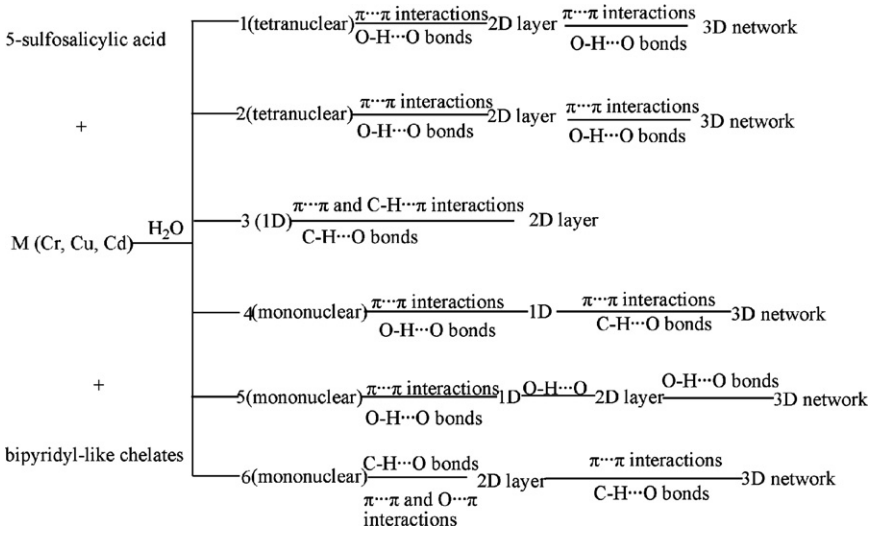

Scheme 2.

4. Conclusion

Six new complexes constructed from 5-sulfosalicylic acid and bipyridyl-like ligands (2,2′-bipy and 1,10-phen), namely $[Cu_4(OH)_2(ssal)_2(phen)_4 \cdot 7H_2O]$ (**1**), $[Cu_4(OH)_2(ssal)_2(bipy)_4 \cdot 2H_2O]$ (**2**), [Cd(Hssal)(bipy)] (**3**), $[Cd(HL)_2(phen)_2]$ (**4**), $[Cr(ssal)(bipy)(H_2O)_2 \cdot 2H_2O]$ (**5**) and $[Cr(ssal)(phen)_2]$ (**6**), (H_3ssal = 5-sulfosalicylic acid, H_2L = *p*-hydroxybenzenesulfonic acid, bipy = 2,2′-bipy, phen = 1,10-phen) were prepared under hydrothermal conditions and their structures were determined by single-crystal X-ray diffraction. Complexes **1** and **2** are both tetranuclear copper complexes with a stepped topology. In complex **3**, a new coordination mode of the $Hssal^{2-}$ group is reported in this work. During the synthetic process of complex **4**, *in situ* decarboxylation of 5-sulfosalicylic acid into *p*-hydroxybenzenesulfonic acid is involved. Two chromium 5-sulfosalicylates (**5** and **6**) are reported for the first time. These new complexes display different supramolecular structures by O–H···O, C–H···O hydrogen bonds as well as π···π, C–H···π and O···π interactions (Scheme 2). Of the six complexes described in this work, the π-stacking interactions (O···π, C–H···π and π···π) play an important role in the observed structural stability. It is likely that studies on similar systems would be favorable for understanding the nature of the π-stacking and its role in structural stability.

Acknowledgement

This work was supported by the National Natural Science Foundation of China (Grant Nos. 20571032 and 20333070).

Appendix A. Supplementary material

CCDC 627686, 627687, 627688, 627689, 627690 and 627691 contain the supplementary crystallographic data for **1**, **2**, **3**, **4**, **5** and **6**. These data can be obtained free of charge via http://www.ccdc.cam.ac.uk/conts/retrieving.html, or from the Cambridge Crystallographic Data Centre, 12 Union Road, Cambridge CB2 1EZ, UK; fax: (+44) 1223-336-033; or e-mail: deposit@ccdc.cam.ac.uk.

X-ray crystallographic files of compounds **1**–**6** in CIF format, a perspective view of the 2D supramolecular layer for complex **1** (S-Fig. 1), the plot of the tetranuclear Cu (II) units included in large rhombic windows consisting of water heptamers and sulfonate anions (S-Fig. 2), the molecular structure of complex **2** (S-Fig. 3), the 2D packing structure of complex **3** (S-Fig. 4), chelating C–H···O hydrogen bonding and C–H···π interactions in complex **3** (S-Fig. 5), 1D supramolecular double chains for compound **4** (S-Fig. 6), the supramolecular ring of the 2D layer in complex **5** (S-Fig. 7), a plot of the 3D supramolecular network for complex **5** (S-Fig. 8), a plot of the 2D supramolecular layer in complex **6** (S-Fig. 9), the mode of O···π and π···π interactions in complex **6** (S-Fig. 10), the plots of the solid-state excitation fluorescent and emission spectra of the 2,2-bipy ligand (S-Fig. 11), phen · H_2O (S-Fig. 12) and H_3ssal · $2H_2O$ (S-Fig. 13) at room temperature. Supplementary data associated with this article can be found, in the online version, at doi:10.1016/j.poly.2007.05.037.

References

[1] G.R. Desiraju, Crystal Engineering: The Design of Organic Solids, Elsevier, Amsterdam, 1989.
[2] (a) S.R. Batten, R. Robson, Angew. Chem., Int. Ed. 37 (1998) 1460;
(b) G.F. Swiegers, J. Malefetse, Chem. Rev. 100 (2000) 3483;
(c) R. Robson, J. Chem. Soc. Dalton Trans. (2000) 3735;
(d) S.R. Batten, CrystEngCommun 3 (2001) 67;
(e) B.J. Holliday, C.A. Mirkin, Angew. Chem., Int. Ed. 40 (2001) 2022;
(f) M. Eddaoudi, D.B. Moler, J. Li, B.L. Chen, T.M. Reineke, M. O'Keeffe, O.M. Yaghi, Acc. Chem. Res. 34 (2001) 319;
(g) C. Janiak, J. Chem. Soc., Dalton Trans. (2003) 2781.

[3] (a) S. Kitagawa, R. Kitaura, S. Noro, Angew. Chem., Int. Ed. 43 (2004) 2334;
(b) L. Brammer, Chem. Soc. Rev. 33 (2004) 476;
(c) N. Malabika, R. Koner, S.E. Helen, M. Sasankasekhar, Cryst. Growth. Des. 5 (2005) 1907;
(d) S.G. Baca, I.G. Filippova, C. Ambrus, M. Gdaniec, Y.A. Simonov, N. Gerbeleu, O.A. Gherco, S. Decurtins, Eur. J. Inorg. Chem. (2005) 3118;
(e) E. Tynan, P. Jensen, A.C. Lees, B. Moubaraki, K.S. Murray, P.E. Kruger, CrystEngCommun (2005) 90;
(f) D. Sunirban, A.M. Simi, P. Satyanarayan, P. Samudranil, Cryst. Growth Des. 9 (2006) 2103.

[4] (a) O.M. Yaghi, H.L. Li, T.L. Groy, J. Am. Chem. Soc. 118 (1996) 9096;
(b) L.Y. Zhang, G.F. Liu, S.L. Zheng, B.H. Ye, X.M. Zhang, X.M. Chen, Eur. J. Inorg. Chem. (2003) 2965;
(c) Y.B. Go, X.Q. Wang, E.V. Anokhina, A.J. Jacobson, Inorg. Chem. 43 (2004) 5360;
(d) A.D. Burrows, R.W. Harrington, M.F. Mahon, S.J. Teat, CrystEngCommun (2005) 388;
(e) W.Z. Shen, X.Y. Chen, P. Cheng, S.P. Yan, B. Zhai, D.Z. Liao, Z.H. Jiang, Eur. J. Inorg. Chem. (2005) 2297;
(f) P. Mahata, S. Natarajan, Eur. J. Inorg. Chem. (2005) 2156;
(g) B. Covelo, R. Carballo, E.M. Vázquez-López, E. García-Martínez, A. Castiñeiras, S. Balboa, J. Niclós, CrystEngCommun (2006) 167;
(h) C.K. Xia, C.Z. Lu, D.Q. Yuan, Q.Z. Zhang, X.Y. Wu, S.C. Xiang, J.J. Zhang, D.M. Wu, CrystEngCommun (2006) 281.

[5] (a) H.Y. Sun, C.H. Huang, X.L. Jin, G.X. Xu, Polyhedron 14 (1995) 1201;
(b) A. Marzotto, D.A. Clemente, T. Gerola, G. Valle, Polyhedron 20 (2001) 1079;
(c) J.F. Li, Y.J. Zhao, X.H. Li, M.L. Hu, Acta Crystallogr. E60 (2004) m1210;
(d) Z.F. Chen, S.M. Shi, R.X. Hu, M. Zhang, H. Liang, Z.Y. Zhou, Chin. J. Chem. 21 (2003) 1059;
(e) E. Hecht, Acta Crystallogr. E60 (2004) m1286;
(f) W.G. Wang, J. Zhang, L.J. Song, J.F. Ju, Inorg. Chem. Commun. 7 (2004) 858;
(g) X.Q. Wang, J. Zhang, Z.J. Li, Y.H. Wen, J.K. Cheng, Y.G. Yao, Acta Crystallogr. C60 (2004) m657.

[6] (a) S.R. Fan, L.G. Zhu, Acta Crystallogr. E61 (2005) m2480;
(b) S.R. Fan, L.G. Zhu, H.P. Xiao, S.W. Ng, Acta Crystallogr. E61 (2005) m377;
(c) W.X. Ma, B.H. Qian, J. Gao, X.Y. Xu, L.D. Lu, X.J. Yang, X. Wang, H.B. Song, Chin. J. Inorg. Chem. 21 (2005) 612;
(d) J.F. Ma, J. Yang, S.L. Li, S.Y. Song, H.J. Zhang, H.S. Wang, K.Y. Yang, Cryst. Growth Des. 5 (2005) 807;
(e) S.R. Fan, L.G. Zhu, Acta Crystallogr. E61 (2005) m174;
(f) S.R. Fan, G.Q. Cai, L.G. Zhu, H.P. Xiao, Acta Crystallogr. C61 (2005) m177;
(g) S.R. Fan, L.G. Zhu, Chin. J. Inorg. Chem. 23 (2005) 1292.

[7] (a) S.R. Fan, H.P. Xiao, L.G. Zhu, Acta Crystallogr. E62 (2006) m18;
(b) B. Liu, Z.J. Wang, S.P. Huang, B.S. Yang, Acta Crystallogr. E62 (2006) m608;
(c) S.R. Fan, L.G. Zhu, Acta Crystallogr. E61 (2005) m2080;
(d) S.R. Fan, L.G. Zhu, H.P. Xiao, Acta Crystallogr. E61 (2005) m804;
(e) F.F. Li, J.F. Ma, S.Y. Song, J. Yang, Cryst. Growth Des. 1 (2006) 209;
(f) Z.D. Lu, L.L. Wen, J. Yao, Z.Z. Zhu, Q.J. Meng, CrystEngCommun (2006) 847;
(g) S.R. Fan, L.G. Zhu, Inorg. Chem. 45 (2006) 7935.

[8] P.V. Khadikar, S. Joshi, S.G. Kashkhedikar, B.D. Heda, Indian J. Pharm. Sci. 46 (1984) 209, and references therein.

[9] (a) X.L. Wang, C. Qin, E.B. Wang, L. Xu, Z.M. Su, C.W. Hu, Angew. Chem., Int. Ed. 43 (2004) 5036;
(b) B.H. Ye, M.L. Tong, X.M. Chen, Coord. Chem. Rev. 249 (2005) 545.

[10] U.W. Grummt, E. Birckner, E. Klemm, D.A.M. Egbe, B. Heise, J. Phys. Org. Chem. 13 (2000) 112.

[11] G.M. Sheldrick, SHELXS97, Program for Crystal Structure Refinement, University of Göttingen, Göttingen, Germany, 1997.

[12] A.L. Spek, PLATON, Molecular Geometry Program, University of Utrecht, The Netherlands, 1999.

[13] (a) I.I. Mathews, H. Manohar, J. Chem. Soc., Dalton Trans. (1991) 2139;
(b) G.A. van Albada, I. Mutikainen, O. Roubeau, U. Turpeinen, J. Reedijk, Inorg. Chem. Acta 331 (2002) 208;
(c) R.L. Lindtvedt, M.D. Glick, B.K. Tomolovic, D.P. Gavel, J.M. Kuszaj, Inorg. Chem. 15 (1976) 1633;
(d) I. Katharina, F. Patrick, A. Christina, B. Gérald, D. Silvio, F.W. Alan, Inorg. Chem. 44 (2005) 3896;
(e) S.H. Gou, M. Qian, Z. Yu, C.Y. Duan, X.F. Sun, W. Huang, J. Chem. Soc., Dalton Trans. (2001) 3232;
(f) Y.Q. Zheng, J.L. Lin, Z. Anorg. Allg. Chem. 628 (2002) 203.

[14] H.F. Zhu, J. Fan, T.A. Okamura, Z.H. Zhang, G.X. Liu, K.B. Yu, W.Y. Sun, N. Ueyama, Inorg. Chem. 45 (2006) 3941.

[15] C. Baes, R.E. Mesmer, The Hydrolysis of Cations, Krieger Publishing Company, Malabar, FL, 1986.

[16] J.P. Jolivet, De la Solution a L'oxyde, Intereditions/CNRS Editions, Paris, France, 1994.

[17] (a) P.U. Maheswari, B. Modec, A. Pevec, B. Kozlevčar, C. Massera, P. Gamez, J. Reedijk, Inorg. Chem. 45 (2006) 6637;
(b) I.A. Gural'skiy, P.V. Solntsev, H. Krautscheid, K.V. Domasevitch, Chem. Commun. (2006) 4808.

[18] W.G. Lu, L. Jiang, X.L. Feng, T.B. Lu, Cryst. Growth Des. 2 (2005) 564.

[19] X. Shi, G.S. Zhu, X.H. Wang, G.H. Li, Q.R. Fang, G. Wu, G. Tian, M. Xue, X.J. Zhao, R.W. Wang, S.L. Qiu, Cryst. Growth Des. 1 (2005) 207.

[20] X. Shi, G.S. Zhu, Q.R. Fang, G. Wu, G. Tian, R.W. Wang, D.L. Zhang, M. Xue, S.L. Qiu, Eur. J. Inorg. Chem (2004) 185.